https://doi.org/10.5194/acp-2022-215
Preprint. Discussion started: 29 March 2022

Atmospheric Chemistry and Physics Discussions

Modelling atmospheric carbonyl sulfide using gross primary productivity to constrain vegetative uptake

Michael P. Cartwright[1,2], Richard J. Pope[3,4], Jeremy J. Harrison[1,2], Martyn P. Chipperfield[3,4], Chris Wilson[3,4], Wuhu Feng[3,5], David P. Moore[1,2] and Parvadha Suntharalingam[6]

[1] School of Physics and Astronomy, Space Park Leicester, University of Leicester, Leicester, UK
[2] National Centre for Earth Observation, Space Park Leicester, University of Leicester, Leicester, UK
[3] School of Earth and Environment, University of Leeds, Leeds, UK
[4] National Centre for Earth Observation, University of Leeds, Leeds, UK
[5] National Centre for Atmospheric Science, University of Leeds, Leeds, UK
[6] School of Environmental Sciences, University of East Anglia, Norwich, UK

Correspondence to: Michael P. Cartwright (mpc24@leicester.ac.uk)

Abstract. We use the TOMCAT 3-D chemical transport model with a balanced flux inventory to simulate the global distribution of atmospheric carbonyl sulfide (OCS). This is compared with limb-sounding satellite observations made by the Atmospheric Chemistry Experiment – Fourier Transform Spectrometer (ACE-FTS) and surface flask measurements made worldwide at 14 National Oceanic and Atmospheric Administration – Earth System Research Laboratory (NOAA-ESRL) sites. By scaling gross primary productivity (GPP) output from the Joint UK Land Environment Simulator (JULES), we provide a new estimation of global OCS vegetative uptake. This is calculated by scaling GPP according to a leaf relative uptake (LRU) term, yielding a global yearly atmospheric uptake of approximately 629 Gg S, which is toward the lower estimates from recent studies. To compensate for this larger vegetative sink, we scale oceanic emissions of OCS up to an annual mean of 689 Gg S, focused over the tropical ocean region. We combine our OCS fluxes to derive a new inventory which was used in a TOMCAT simulation from 2004-2018 to allow and investigate the annual distribution and seasonality of OCS as well as long term comparisons with available measurements. The simulation matches satellite and surface observations to within their uncertainties in most instances. When compared to co-located ACE-FTS OCS profiles between 5 km and 30 km, the simulation remains within 5% of the measurements throughout the majority of this region and lies within the standard deviation of these measurements. At the surface, the model captures background concentrations at most of the surface sites to within the maximum and minimum of the seasonal measurements. Compared to a control TOMCAT simulation using the existing Kettle et al. (2002) benchmark flux inventory, errors in the surface comparisons are reduced by as much as 57%. Our new inventory reduces the average difference in the modelled seasonal amplitude compared to the surface measurements from ±40% to ±34%. Other key improvements include better representation of OCS seasonality at North Hemisphere continental sites, as well as a better match in background concentration at tropical Hawaiin sites.

https://doi.org/10.5194/acp-2022-215
Preprint. Discussion started: 29 March 2022

Atmospheric Chemistry and Physics Discussions

1 Introduction

Carbonyl sulfide (OCS) is the most abundant of all sulfur-containing gases in the atmosphere and is important due to its potential use as a proxy for the photosynthetic uptake of carbon dioxide (CO_2) by vegetation (Sandoval-Soto and Stanimirov, 2005; Montzka et al., 2007; Campbell et al., 2008; Suntharalingam et al., 2008; Blonquist et al., 2011; Berry et al., 2013; Launois et al., 2015b). Furthermore, due to its oxidation in the stratosphere, OCS is the largest source of sulfuric acid in the stratospheric aerosol layer in times of low volcanic activity (Crutzen, 1976; Kremser et al., 2016). In the troposphere OCS has a global mean mixing ratio (mole fraction) of approximately 480 parts per trillion (ppt) with a lifetime of approximately 2.5 years (Montzka et al., 2007). In the stratosphere the OCS mixing ratio declines strongly with increasing altitude with a longer mean lifetime of 64 ± 21 years (Barkley et al., 2008).

While Kremser et al. (2015) showed positive OCS trends between 2001 and 2015, determined from ground-based Fourier transform spectrometer column measurements, that study was limited to 3 southern hemisphere (SH) sites. In contrast, the National Oceanic and Atmospheric Administration - Earth System Research Laboratory (NOAA-ESRL) global monitoring network has 14 sites and shows no consistent trend in surface OCS at any one location during the period of 2000 to 2005 (Montzka et al., 2007). Furthermore, Glatthor et al. (2017) concluded that the tropospheric OCS budget is balanced based on a global Michelson Interferometer for Passive Atmospheric Sounding (MIPAS) satellite dataset (2002-2012), while ground-based partial-column measurements at the Jungfraujoch (46.5°N, 8.0°E) showed no significant trend between 2008 and 2015 (Lejeune et al., 2017). In this study we aim to quantify the global atmospheric OCS budget, which is considered balanced, including all sources and sinks, using observations and modelling techniques.

The main source of atmospheric OCS is oceanic emission, with total estimates ranging from 230 to 992 Gg S yr^{-1} (Kettle et al., 2002; Montzka et al., 2007; Suntharalingam et al., 2008; Berry et al., 2013; Glatthor et al., 2015; Launois et al., 2015a; Lennartz et al., 2021; Ma et al., 2021). Oceanic emission has 3 main contributions: direct emission of OCS, oxidation of emitted dimethyl sulphide (DMS) and oxidation of emitted carbon disulphide (CS_2). Both light-dependent (photochemical) and light-independent production play a role in oceanic emission (Launois, et al., 2015a), a large portion of which is driven by biological production (Lennartz et al., 2021). Furthermore, Lennartz et al. (2021) suggest the importance of ocean-emitted OCS and CS_2 exceeds that of DMS which accounts for only a small portion of overall OCS oceanic emissions.

Vegetative uptake is the most important atmospheric sink of OCS, and its magnitude is significantly more uncertain than the ocean flux, with estimates ranging from 210 to 2400 Gg S yr^{-1} (Kettle et al., 2002; Sandoval-Soto and Stanimirov, 2005; Suntharalingam et al., 2008; Berry et al., 2013; Glatthor et al., 2015; Kuai et al., 2015; Launois et al., 2015b; Ma et al., 2021). OCS is consumed during the photosynthesis process, which proceeds along the same enzymatic pathways as CO_2 (Protoschill-Krebs and Kesselmeier, 1992). However, unlike for CO_2, this process is one-way due to the irreversible OCS hydrolysis reaction, catalysed by carbonic anhydrase (Protoschill-Krebs et. al, 1996). OCS hydrolysis also occurs in soil, again catalysed by carbonic anhydrase (Kesselmeier et al., 1999; Li et al., 2005; Seibt et al., 2006; Kato et al., 2008), which is the second largest OCS sink, with an estimated annual loss of 127-355 Gg S (Kettle et al., 2002; Montzka et al., 2007; Berry et al., 2013;

https://doi.org/10.5194/acp-2022-215
Preprint. Discussion started: 29 March 2022


Atmospheric Chemistry and Physics Discussions

Glatthor et al., 2015; Kuai et al., 2015). Other findings suggest that the seasonal variation in OCS soil uptake is relatively weak in boreal forest regions, but shows dependency on soil moisture (Sun et al., 2018). Soil has also been observed to act as an emitter of OCS in warm conditions (Maseyk et al., 2014).

Chin and Davis (1993) presented one of the first attempts at quantifying global OCS (and CS_2) budget terms, but these were subject to substantial uncertainties. However, multiple terms, such as atmospheric loss and volcanism, were subsequently used in the estimates presented by Watts (2000) and Kettle et al. (2002), the latter of which has been used as a benchmark for more recent studies. Analysis of flask and aircraft data spanning both hemispheres by Montzka et al. (2007) have offered the most significant updates since the aforementioned studies and suggests a vegetative sink (1115 Gg S yr^{-1}) up to five times larger than the estimate (240 Gg S yr^{-1}) presented by Kettle et al. (2002). Due to the negligible atmospheric OCS trend, this would suggest a larger source is required for balance. The general consensus is that this must originate in the tropical oceans, due to measurement peaks from satellite and aircraft observations (Glatthor et al., 2015; Kuai et al., 2015), as well as modelling estimates pointing to this region as an underestimated source (Berry et al., 2013; Launois et al., 2015a). There is opposition from Lennartz et al. (2017), who estimate global oceanic emissions to be approximately 350 Gg S yr^{-1}, derived using a global oceanic box model and measurements of surface waters, thus too low to account for this difference entirely. Subsequently Ma et al. (2021) acknowledges the need for a larger tropical source or weaker sink(s) but downplays the likelihood if it being of exclusively oceanic origin. A recent study has also suggested there is an underestimation in previous gridded anthropogenic OCS flux inventories by 200 Gg S yr^{-1}, which could account for some of the deficit (Zumkehr et al., 2018). These recent studies quantifying OCS flux inventories show less uncertainty than previous ones. However, to improve the inventories further, increased spatial coverage by ground-based and remote atmospheric OCS observations are required, as well as OCS flux measurements (Whelan et al., 2018).

In this study we evaluate the suitability of gross primary productivity to estimate the OCS vegetative uptake. An array of prescribed fluxes is used for the remainder of the budget, mostly derived from Kettle et al. (2002), some of which are scaled according to findings from other studies, and to bring the budget into balance (Suntharalingam et al., 2008; Berry et al., 2013; Kuai et al., 2015; Ma et al., 2021). This new inventory of OCS fluxes is used to drive the TOMCAT 3-D chemical transport model (CTM) over the time period 2004 - 2018, to provide fresh insight that improves our understanding of the magnitude and location of fluxes of OCS. Sect. 2 summarises the data used for evaluating the model. The model setup and flux inventory are described in Sect. 3. Results and comparisons with tropospheric and stratospheric satellite observations from the ACE-FTS instrument (Bernath, 2017) and measurements made by the NOAA-ESRL flask network (Montzka et al., 2007) are shown in Sect. 4, discussed further in in Sect. 5 and concluding remarks presented in Sect. 6.

https://doi.org/10.5194/acp-2022-215
Preprint. Discussion started: 29 March 2022


Atmospheric Chemistry and Physics Discussions

2 Observations

2.1 Atmospheric Chemistry Experiment – Fourier Transform Spectrometer (ACE-FTS) Observations

Onboard the SCISAT satellite, launched in August 2003, is the Atmospheric Chemistry Experiment infrared Fourier transform spectrometer (ACE-FTS), which operates in a solar occultation mode measuring radiation between 750 and 4400 cm^{-1} at a spectral resolution of 0.02 cm^{-1} (Bernath et al., 2005; Bernath, 2017). Atmospheric trace gas profiles are retrieved using a non-linear least squares global-fit approach on the measurement altitude grid (3 km vertical resolution), then interpolated on to a uniform 1 km grid. ACE-FTS is capable of measuring profiles for a number of trace gases, including OCS from 5 km (or cloud top) up to about 30 km. OCS is retrieved using microwindows of various widths between 2039.01 and 2057.52 cm^{-1}, including a band at 1950.10 cm^{-1} to minimise the impact of H_2O interference. Because the primary science mission of ACE-FTS is to measure atmospheric ozone distributions over Canada, the satellite's orbit is such that approximately 60% of all measurements are at latitudes poleward of ±60°. However, over the course of a year measurements are taken over a wide range of latitudes, providing a wealth of data with which to validate global CTM simulations. For this study, ACE-FTS version 4.1 (hereafter ACE) retrieved profiles from February 2004 to December 2018 (approximately 98,000 profiles) (Boone et al., 2020) were used in the validation of the modelled TOMCAT OCS distribution. The version 4.1 retrievals incorporate a new instrumental line shape (Boone and Bernath, 2019) and utilise the 2016 HITRAN data (Gordon et al., 2017). While the planned ACE mission duration was only two years, it now has a data record spanning 18 years. This longevity makes the ACE-FTS a valuable tool for measuring atmospheric trace gases and characterising their variability and trends.

2.2 NOAA-ESRL Flask Measurements

The surface OCS measurements described here are shown in Sect. 4; here we present a summary of the method of data collection and the site information (see Table 1). Flasks of ambient air have been collected approximately 1 to 5 times per month at 14 measurement sites across both hemispheres since early 2000. Measurements of the OCS concentrations within the flasks are made using gas chromatography and mass spectrometry at the NOAA-ESRL Boulder laboratories (Montzka et al., 2007). In this study we use data from all the Halocarbons & other Atmospheric Trace Species (HATS) surface measurement sites for the purpose of validating the surface OCS concentrations from the TOMCAT model.

https://doi.org/10.5194/acp-2022-215
Preprint. Discussion started: 29 March 2022


Atmospheric Chemistry and Physics Discussions

Table 1. NOAA-ESRL flask sampling site information for OCS measurements.

Code	Name	Country	Latitude (°N)	Longitude (°E)	Elevation (metres)
ALT	Alert, Nunavut	Canada	82.5	-62.5	185
BRW	Barrow, Alaska	United States	71.3	-156.6	11
CGO	Cape Grim, Tasmania	Australia	-40.7	144.7	94
HFM	Harvard Forest, Massachusetts	United States	42.5	-72.2	340
KUM	Cape Kumukahi, Hawaii	United States	19.7	-155.0	0.3
LEF	Park Falls, Wisconsin	United States	45.9	-90.3	472
MHD	Mace Head, County Galway	Republic of Ireland	53.3	-9.9	5
MLO	Mauna Loa, Hawaii	United States	19.5	-155.6	3397
NWR	Niwot Ridge, Colorado	United States	40.1	-105.6	3523
PSA	Palmer Station	Antarctica	-64.8	-64.1	10
SMO	Tutuila	American Samoa	-14.2	-170.6	42
SPO	South Pole	Antarctica	-90.0	-24.8	2810
SUM	Summit	Greenland	72.6	-38.4	3209
THD	Trinidad Head, California	United States	41.1	-124.2	107

3 Chemical transport modelling of OCS

3.1 TOMCAT Model Setup

We have used the TOMCAT 3-D off-line CTM (Chipperfield, 2006) to model atmospheric OCS. This model has been used in a wide range of studies, including recently to better constrain methane flux estimations (Wilson et al., 2016; Parker et al., 2018), as a forward model for methane flux inversions (McNorton et al., 2018) and to investigate stratospheric ozone depletion

https://doi.org/10.5194/acp-2022-215
Preprint. Discussion started: 29 March 2022


Atmospheric Chemistry and Physics Discussions

(Claxton et al., 2019). In this work, TOMCAT is driven by meteorological reanalysis data (ERA-Interim) from the European Centre for Medium-Range Weather Forecasts (ECMWF, Dee et al., (2011)). ERA-Interim convective mass fluxes are used following the scheme presented in Feng et al. (2011). The model distribution of OH is specified from pre-computed fields which vary monthly, but not inter-annually. The monthly distributions are taken from Spivakovsky et al. (2000) and scaled by a factor of 0.92 in accordance with Huijnen et al. (2010). The photolysis loss is based on precomputed rates from the full chemistry version of TOMCAT (Monks et al., 2017). TOMCAT is spun for 10 years prior to 2004, and then run between 2004 and 2018 at a horizontal resolution of approximately 2.8° × 2.8° (T42 Gaussian grid), with 60 atmospheric layers from the surface up to 0.1 hPa. The geopotential height output from the model is converted to altitude for ease of comparison to ACE-FTS; this is done using the hypsometric equation at a reference pressure of 1000 hPa, and then interpolated on to the 1 km equidistant altitude grid used by ACE-FTS. Furthermore, the profiles outputted by TOMCAT are spatio-temporally co-located with the ACE-FTS observations to provide a precise like-for-like comparison. Surface emission fields of OCS were implemented within TOMCAT on a monthly 1° × 1° grid with no inter-annual variability and comprise nine fluxes: six sources and three sinks. These are mapped onto the model grid in a way that conserves local distributions and the total global flux.

3.2 OCS Flux Inventory

The fluxes described here originated from the literature (Watts, 2000; Kettle et al., 2002; Suntharalingam et al., 2008), and are used to run a control simulation, denoted $TOMCAT_{CON}$. This model run is utilised as a comparison to the model driven by our new inventory of fluxes described in Sect. 3.3 and Sect. 3.4 ($TOMCAT_{OCS}$).

Three of the six sources used in the model are oceanic: a direct OCS flux term, one due to oxidation of CS_2 and one due to oxidation of DMS. These were converted to OCS emissions using molar conversion factors (Chin and Davis, 1993; Barnes et al., 1994). The OCS and CS_2 emission terms were quantified using a physio-chemical model, the main source being from photochemical production (Kettle et al., 2002). However, as DMS measurements are more abundant than OCS and CS_2, these were used to parameterize this flux (Kettle and Andreae, 2000). Anthropogenic OCS emissions consist of two factors, a direct term and one from the oxidation of CS_2, the latter being considerably larger. Eleven anthropogenic sources of OCS were an quantified by Zumkehr et al. (2018) for the period 1980 – 2012, the largest contributions originating from residential and industrial coal usage and the rayon industry. Emission factors for each source are applied to country-scale industrial activity data, obtained from a wide range of sources, then gridded spatially and temporally based on a gridded proxy flux (Zumkehr et al., 2018). The final source term is biomass burning scaled similarly to that in Kettle et al. (2002), but varies according to the monthly climatology of Duncan et al. (2003).

The three sink terms are an oceanic sink, soil uptake and a vegetative sink. The first was quantified using the same physio-chemical model used for the OCS and CS_2 source terms described above and covers the periods in the year where the direct oceanic emission of OCS flips from being a source to becoming a sink. These are focused mostly over extra-tropical open ocean regions and during each hemisphere's summer period. Gridded soil uptake was calculated by applying correction factors for temperature, ambient OCS and soil water content to a standardised uptake rate of 10 pmol m^{-2} s^{-1} (Kesselmeier et. al, 1999).

https://doi.org/10.5194/acp-2022-215
Preprint. Discussion started: 29 March 2022


Atmospheric Chemistry and Physics Discussions

The monthly mean climatological data for the temperature and soil water content is taken from Sellers et al. (1995), where the soil water content is a percentage of saturation in the top 2 cm of soil. Anoxic soil emissions are neglected in this study. Finally, the vegetative uptake is calculated by employing a normalised difference vegetation index (NDVI) to scale net primary productivity (NPP) distribution from Fung et al. (1987).

3.3 Calculating OCS Vegetative Uptake using Gross Primary Productivity

The new vegetative sink calculation in this work differs fundamentally from the method described in Sect. 3.2, and used in the control model simulation, as the use of NPP has been shown to underestimate the seasonal amplitude in other modelling studies (Suntharalingam et al., 2008; Berry et al., 2013). Sandoval-Soto and Stanimirov (2005) suggested that using NPP to calculate OCS uptake would underestimate the global burden and therefore they recommend using gross primary productivity (GPP) as an alternative. Furthermore, they were the first to quantify deposition velocity ratios for CO_2 and OCS for different plant types, which previous studies had assumed to be equal.

$$F_{OCS} = GPP \frac{[OCS]}{[CO_2]} \times LRU, \quad (1)$$

Using Eq. (1) we calculated the vegetative flux of OCS (F_{OCS}) by scaling GPP using a leaf relative uptake (LRU) of 1.6 (Stimler et al., 2012). This LRU value was a mean value from gas-exchange measurements of 22 plant species (Stimler et al., 2012), which is a necessary simplification until more sophisticated land surface models and measurements of OCS plant uptake are available. LRU is the normalised ratio of OCS assimilation rates to CO_2 at the leaf-scale. This is then normalized by background concentrations of the two gases, signified by the square brackets in Eq. (1). The GPP flux used in our calculation, generated by the Joint UK Land Environment Simulator (JULES) model, applies the WATCH Forcing Data methodology to ERA-Interim reanalysis (WFDEI) between 1979 and 2012 and uses Global Precipitation Climatology Centre (GPCC) precipitation data (Slevin et al., 2016). Here we used only monthly data for 2010, as the interannual variability in the amplitude of the GPP cycle is only about 1% (Chen et al., 2017). Monthly mean gridded CO_2 surface mixing ratios for 2010 from a TOMCAT simulation which assimilated surface flask observations of CO_2 (Gloor et al., 2018) are used for the background CO_2. Our resulting estimate of the mean global yearly value of F_{OCS} between 2004 and 2018 is 629 Gg S, which is nearly three times the value of Kettle et al. (2002), 240 Gg S, but is slightly under half that of the largest estimation of 1115 Gg S in Table 2 from Montzka et al. (2007).

3.4 Balancing the OCS Budget

To balance the OCS budget, under the assumption of a larger vegetative uptake term than that of Kettle et al. (2002) (Sect. 3.3), we scale several of the emission terms described in Sect. 3.2, although some of the difference was accounted for in the larger anthropogenic emissions. Furthermore, some of the fluxes were adjusted to better represent recent estimations in the literature.

https://doi.org/10.5194/acp-2022-215
Preprint. Discussion started: 29 March 2022


Atmospheric Chemistry and Physics Discussions

The soil flux included in this study was calculated by Kettle et al. (2002) using the method described in Sect. 3.2 and assumes a constant 500 ppt OCS ambient value in the scaling of the standardised uptake. Soil uptake was scaled by 2.5 times from 130 Gg S yr^{-1} to 322 Gg S yr^{-1} to bring it in line with literature findings that estimate soil uptake to be between 355 – 507 Gg S yr^{-1} (Berry et al., 2013; Launois, 2015b). These studies used different approaches; Berry et al. (2013) use a global carbon cycle model, SiB 3, to obtain a new estimate of soil uptake based on empirical data and a mechanistic understanding of the processes influencing OCS diffusion into soil. Launois et al. (2015b) use H_2S soil deposition to infer OCS, as this is a by-product of the OCS hydrolysis reaction and therefore a proxy for OCS.

Suntharalingam et al. (2008) recommend a reduction in direct OCS and indirect OCS emissions from DMS by 40% (as this yielded the smallest root-mean-squared error in their analysis) in SH mid-latitude (ML) and high-latitude (HL, here defined as 60° – 90°) regions, due to improvements to the seasonal cycle at Antarctic NOAA-ESRL sites. They also implemented an enhanced OCS tropical ocean source that was aseasonal and uniform across the tropics. However, here we scale up the CS_2 source term to 439 Gg S yr^{-1} to balance the increased vegetation and soil sink terms discussed above and bring the net budget to near balance. We scaled this flux not necessarily because it was suspected that CS_2 was the erroneous term in the OCS budget, but because it is more realistic to add a flux that is focused spatially over the tropical region already (Kuai et al., 2015). The reason for this geographical distribution is that CS_2 emissions are proportional to temperature and incident solar radiation, hence why the tropics show the strongest emissions (Kettle et al., 2002).

Initial testing of our new fluxes in TOMCAT yielded low-biased simulated OCS concentrations at Northern Hemisphere (NH) NOAA-ESRL sites, but a seasonal cycle with appropriate amplitude (not shown). To improve the agreement, the direct and indirect OCS terms arising from DMS were increased by a factor of 2. These fluxes were chosen as their spatial distribution includes peaks in the Northern Atlantic and Pacific regions. When including the reduction implemented for these terms in the Southern Ocean, the global net increase for direct OCS and indirect OCS from DMS is roughly 10 Gg S yr^{-1} and 7 Gg S yr^{-1}, respectively, which is relatively small compared to the changes to the vegetative, soil and oceanic CS_2 fluxes.

Scaling OCS emitted from biomass burning and anthropogenic sources was not considered suitable to balance increases to sink terms, as these are less uncertain than oceanic emissions. Furthermore, biomass burning is more focused in lower latitude agricultural regions and anthropogenic emissions tend to be focused over point sources, mostly in Asia.

Using the flux inventory described here, TOMCAT OCS simulations were carried out covering 2004 to 2018, initialised at 500 ppt in every grid-box and spun up for 10 years between 1994 and 2004. Average yearly burdens for 2004 to 2018 yield a broadly closed OCS budget. Inter-annual variability in meteorology will have an impact on the model's ability to have a mean closed budget over the full time period. The vegetative flux sits roughly in the middle of literature estimates, but the total sink term is similar to larger estimates from Berry et al. (2013), Kuai et al. (2015) and Ma et al. (2021), as seen in Table 2, as well as estimates from Glatthor et al. (2015) and Launois et al. (2015b), not shown in Table 2. Atmospheric destruction, mainly in the form of stratospheric loss from OH and photolysis reactions, account for approximately 154 Gg S yr^{-1} removal, which is 25% larger than fields used in earlier studies in Table 2, of roughly 126 Gg S yr^{-1}, derived by Watts (2000). The total oceanic emission has been increased 146% from the starting point of Kettle et al. (2002); the majority of this increase is focused in the

https://doi.org/10.5194/acp-2022-215
Preprint. Discussion started: 29 March 2022


Atmospheric Chemistry and Physics Discussions

tropical region. With a global net annual emission of 1141 Gg S, roughly equal to that of our sink terms, the model yields 14 years of broadly balanced OCS budget, with all terms in line with the findings of recent studies (Berry et al., 2013; Glatthor et al., 2015; Kuai et al., 2015; Launois et al., 2015a; Ma et al., 2021).

225

https://doi.org/10.5194/acp-2022-215
Preprint. Discussion started: 29 March 2022

Atmospheric Chemistry and Physics Discussions

Table 2. Global OCS budgets (units Gg S yr^{-1}). Values for past studies are an average of the upper and lower limits stated in those studies, unless a value is stated exactly. Values for this study are an average between 2004 and 2018.

Source/Sink Process	Kettle et al. (2002)	Montzka et al. (2007)	Suntharalingham et al. (2008)	Berry et al.[a] (2013)	Kuai et al.[b] (2015)	Ma et al.[c] (2015)	**This Study**
Vegetation	-238	-1115	-490	-738	-775	-1053	-629
Oxic Soil	-130	-127	-120	-355	-176		-322
Reaction with OH	-94	-96		-101	-111	-101	-122
Reaction with $O(^1D)$	-11	-11	-130	0	0	0	0
Photolysis	-16	-16		0	0	-40	-32
Ocean	0	0	0	0	0	0	-39
Total Sinks	-489	-1365	-740	-1194	-1062	-1194	-1144
Ocean (OCS)	41	40				40	
Ocean (CS_2)	84	240	230	876	838	81	689
Ocean (DMS)	154					156	
Total Ocean Emission	279	280	230	876	838	277	689
Anthropogenic (OCS)	64	64		64	62	155	410
Anthropogenic (CS_2)	116		180	116	113	188	
Anthropogenic (DMS)	1	0		1		6	0
Total Anthropogenic Emission	181	64	180	181	175	349	410
Biomass Burning	38	106	70	136	49	136	42
Other (mainly wetlands & anoxic soils)	26	66	25	0	0	425	0
Total Sources	523	516	505	1193	1062	1187	1141
Net Budget	34	-849	-235	-2	0	-6	-3

[a]Ocean emission term includes an additional photochemical oceanic flux of 600 Gg S.

[b]Ocean emission term includes an additional evenly distributed ocean term of 559 Gg S.

[c]Posterior estimates from the Su inversion are shown here. An 'unknown' term is used to quantify a missing source in the inversion, this is included in 'other' in Table 2.

https://doi.org/10.5194/acp-2022-215
Preprint. Discussion started: 29 March 2022


Atmospheric Chemistry and Physics Discussions

4 Results

Output from model runs using the flux inventory and F_{OCS} calculations described in Sect. 3.3 and 3.4, hereafter referred to as $TOMCAT_{OCS}$, and $TOMCAT_{CON}$, are compared with NOAA-ESRL surface flask observations, by co-locating the nearest grid box and time step. $TOMCAT_{OCS}$ is also co-located and compared to ACE, which has approximately 98,000 profiles in the modelled time period, all of which are filtered for outliers before analysis, as described in Sect. 3.1. As ACE measures the upper troposphere and stratosphere primarily, this region is less sensitive to surface processes, so we only compare the main simulations.

4.1 Seasonality of Modelled OCS compared to Surface Flask Measurements

TOMCAT simulates OCS distributions down to the surface, where the majority of OCS fluxes occur; it is therefore important that the model performs well at this level. A control model simulation ($TOMCAT_{CON}$) using fluxes from Kettle et al (2002) (with the vegetative sink scaled to the quoted upper limit of 270 Gg S yr^{-1}) is presented here to provide further comparison with $TOMCAT_{OCS}$. $TOMCAT_{CON}$ was initialised using OCS values in each grid box from $TOMCAT_{OCS}$, after 10 years (1994 – 2003) spin-up. Only 2004 monthly mean mixing ratios from $TOMCAT_{CON}$ have been included, as this flux inventory has a net negative budget and therefore a negative trend over longer periods.

Figure 1 compares the seasonal cycles of NOAA-ESRL surface flask measurements (black) with $TOMCAT_{OCS}$ (blocked-blue), and $TOMCAT_{CON}$ (orange) simulations. As $TOMCAT_{CON}$ was only run for 2004, a blue dashed line representing 2004 of $TOMCAT_{OCS}$ is also indicated ($TOMCAT_{OCS\_2004}$). NOAA-ESRL flask measurements between 2004 and 2018 are from 14 sites, 4 in the SH and 10 in the NH (see Table 1). Error bars associated with the observations represent the maximum and minimum values for each month at every site. The modelled vertical layer of $TOMCAT_{OCS}$ and $TOMCAT_{CON}$ closest to the altitude of the measurement site was used for closer comparison because the bottom-most model layer does not necessarily correspond with the surface due to the relative coarseness of model grid boxes affecting the simulated surface topography. Comparisons between $TOMCAT_{OCS}$ and $TOMCAT_{CON}$ are shown here to emphasise the improvements made by the flux inventory developed in this study. The root mean square error (RMSE) for the entire period is shown for each site, alongside the seasonal cycle amplitude (SCA). Generally, there is an improvement in RMSE across all the sites, but in some cases, there is a degradation, which is mostly attributed to background concentration, rather than the model's ability to capture a suitable seasonal cycle, hence both are shown.

The fluxes used to model $TOMCAT_{OCS}$ reduces the RMSE from an annual mean of 24.3 to 21.2 ppt for all sites, an error reduction of 3.1 ppt (12.5%), compared to $TOMCAT_{CON}$. This improves to 5.1 ppt (20.4%) if we are to exclude MHD, a particularly poorly represented site according to this metric. Furthermore, SCA is improved from a mean difference to the observations of ±30.5 ppt (40.4%) in $TOMCAT_{CON}$ to ±26.5 ppt (33.6%) in $TOMCAT_{OCS}$. These metrics suggest that the flux inventory used in $TOMCAT_{OCS}$ offers an improvement in capturing seasonality and observation representation at the surface.

https://doi.org/10.5194/acp-2022-215
Preprint. Discussion started: 29 March 2022


Atmospheric Chemistry and Physics Discussions

The surface observations show that OCS concentrations peak in April or May in the NH and reach a minimum in September, which is consistent in all 10 NH sites. This seasonal cycle resembles that of CO_2, hence GPP is a suitable proxy for calculating OCS uptake. Despite several of the NH sites being particularly far north, photosynthesis is still the dominant driving flux, which emphasises the strength of the OCS vegetative uptake signal.

Relative to the flask measurements, the SCA at the 8 NH continental measurement sites (top 8 plots in Fig. 1) is captured well by $TOMCAT_{OCS}$, but less so by $TOMCAT_{CON}$. At all sites there is some improvement, except for BRW, which shows little change, but an improved RMSE, and MHD which shows an overestimated SCA by 39.0%. $TOMCAT_{CON}$ shows some instances of peak OCS occurring in March or February in the NH continental sites (LEF, HFM, SUM), which is several months earlier than the observations. SCA is underestimated in $TOMCAT_{CON}$ output at all 8 of these sites by a mean amount of roughly 38.8 ppt. $TOMCAT_{OCS}$ improved this disparity to a net difference of 36.9 ppt (MHD is overestimated). The site showing the largest improvement in RMSE is NWR which sees a 51% error reduction compared to $TOMCAT_{CON}$ and the most improved SCA compared to $TOMCAT_{CON}$ is LEF, which increases SCA by 17.2%, reducing the difference to NOAA-ESRL from 47.4% to 38.3% underestimation.

LEF and HFM are dense woodland sites and have particularly large SCA which can often be a challenge for models to simulate. Here we show realistic amplitudes in the seasonal cycle from $TOMCAT_{OCS}$, 76 ppt at LEF and 71 ppt at HFM, compared to observed values of 123 ppt and 128 ppt, respectively. While it does underestimate the full seasonal amplitude, the model still sits within the range of values measured at these sites between 2004 and 2018. The underestimation in $TOMCAT_{OCS}$ could potentially be attributed to using a single value for the LRU parameter globally, as this value is known to vary significantly between plant types (Stimler, et al., 2012). Alternatively, the cause of the underestimation could originate, at least in part, from an underestimation in GPP in this geographical region.

ALT, SUM and BRW are located at high northern latitudes, where the landscape has significantly less vegetation and is more homogeneous than at LEF and HFM, although the seasonal cycle is still driven by typical NH processes. Phasing of the peak and trough of the annual seasonal cycles at ALT, SUM and BRW are improved in $TOMCAT_{OCS}$ output, compared to $TOMCAT_{CON}$, but RMSE and SCA are not improved significantly. THD and MHD are both coastal sites and the misalignment in observed and modelled seasonal cycles could be attributed to the impact from the ocean fluxes in the model grid boxes. Additionally, capturing the seasonal cycle of trace gases at a site such as MHD can be particularly challenging as there are significant seasonal changes in advected airmasses.

At particularly high-altitude sites, NWR and MLO, Fig. 1 shows that $TOMCAT_{OCS}$ underestimates the background concentration and showing no significant improvement in SCA from $TOMCAT_{CON}$. The measured SCA at SUM is 98 ppt (526 ppt to 428 ppt), which is modelled relatively poorly by $TOMCAT_{CON}$, 54.8 ppt, and improved by $TOMCAT_{OCS}$ to 60.1 ppt. A significant difference between SUM and the other two locations is that the topography in the grid boxes for NWR and MLO is very spatially variable; for example, MLO is a high volcano on a relatively small island in the Pacific Ocean. These results suggest the model underestimates OCS concentration around 1 – 3 km above sea level and there is little improvement between $TOMCAT_{OCS}$ and $TOMCAT_{CON}$.

https://doi.org/10.5194/acp-2022-215
Preprint. Discussion started: 29 March 2022


Atmospheric Chemistry and Physics Discussions

Two NH tropical sites, MLO and KUM, exhibit a seasonal cycle in the measurements similar to that of NH continental sites, with slightly different phasing and a reduced seasonal amplitude, which is due to influence of oceanic processes. Conversely, SMO, in the SH tropics, is more dominated by ocean processes and peaks earlier in the year. $TOMCAT_{OCS}$ at MLO, KUM and SMO show varying levels of agreement with the observations, KUM RMSE is reduced by 56.8% and reduced the absolute SCA difference by 80%, from 17.7 Gg ppt to 3.4 ppt, when compared to $TOMCAT_{CON}$. MLO and SMO background concentration is better represented by $TOMCAT_{OCS}$, both observing RMSE improvement of -45.8% and -30.2%, respectively, but the seasonality is out of phase with the observations, peaking approximately 1 month too late, while KUM is 2 months late. A challenge in diagnosing the misalignment in the Hawaii sites is their proximity to the ocean, as the 2.8° × 2.8° grid box is dominated by oceanic flux, as are all the boxes around it. $TOMCAT_{CON}$ shows an improvement in the SCA and phasing of the OCS seasonality in the tropics, which can be attributed to the enhanced oceanic source, which clearly drives the annual variability.

All four SH sites SMO, CGO, PSA and SPO show lower SCA in the observations than all NH sites, ranging from 25 ppt at SMO to 45 ppt at PSA, which is 80% and 65% less variation, respectively, than the forested site HFM. This emphasises the impact vegetation has on NH OCS seasonal cycle. Unlike SMO, the latter 3 sites are dominated much more by oceanic fluxes peaking in SH summer due to the association of phytoplankton growth with OCS emissions, driven by solar radiation. The background concentration of OCS is captured well by $TOMCAT_{OCS}$ and $TOMCAT_{CON}$ at CGO, PSA and SPO, all generally sitting within the maximum and minimum flask measurements (black error bars in Fig. 1), but the seasonal amplitude is overestimated in both the model runs for all three sites. $TOMCAT_{OCS}$ overestimates the SCA at CGO, SPO and PSA, compared to the flask measurements by 5.1 ppt, 6.1 ppt and 33.6 ppt, respectively. In contrast, $TOMCAT_{CON}$ overestimates by 18.2 ppt, 43.2 ppt and 11.8 ppt respectively. This suggests the reduction in Southern Oceanic emissions in $TOMCAT_{OCS}$ improves seasonality in OCS adequately but could be reduced further.

https://doi.org/10.5194/acp-2022-215
Preprint. Discussion started: 29 March 2022

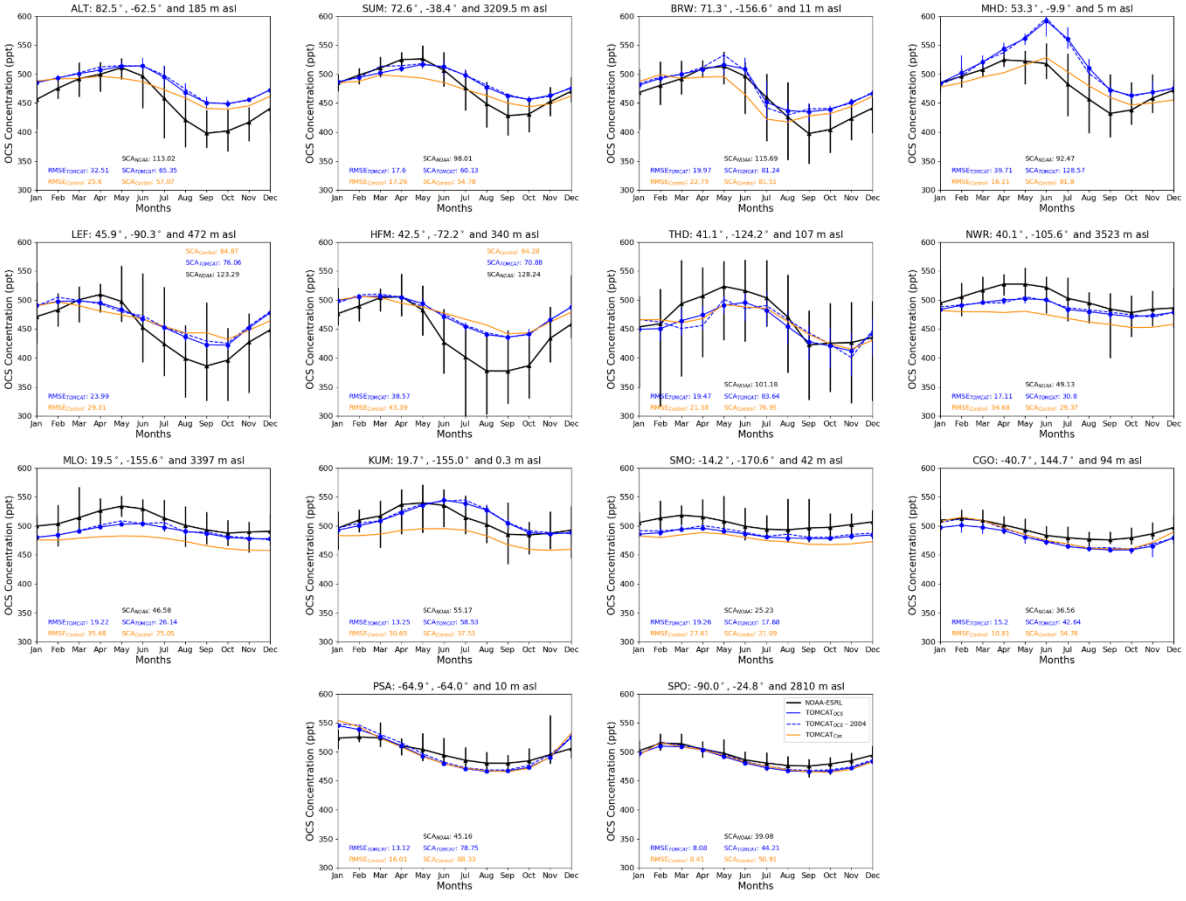

Figure 1. Monthly mean OCS concentration (in ppt) at NOAA-ESRL flask sites (black lines) compared with TOMCAT$_{OCS}$ (blocked-blue line) for the 2004 to 2018 period. The dashed blue line is just 2004 for the TOMCAT$_{OCS}$ dataset and is compared to TOMCAT$_{CON}$ (orange lines). Geographical location of each site is referenced in the titles. Altitude above sea level (asl) of the site is stated and nearest level in TOMCAT used for comparison.

4.2 Spatial Distribution of Modelled OCS compared to Satellite Observations

Figure 2 shows the spatial distribution of atmospheric OCS obtained by averaging ACE profiles across all longitudes and in 5° latitude bins (central column), along with the TOMCAT$_{OCS}$ profiles averaged in the same way (left column). The difference between the two datasets is shown in the right column (TOMCAT$_{OCS}$ minus ACE). ACE-FTS is capable of measuring at altitudes between 6.5 km and 30.5 km, depending on latitude. Figure 2 shows that ACE tropospheric OCS mixing ratios (middle column) range from 425 to 500 ppt, peaking in the upper troposphere-lower stratosphere (UTLS) region, which extends from about 7 km in the NH ML and up to 17 km in the tropics. OCS values decline above and below the UTLS due to removal by photosynthesis at the surface and photochemistry in the stratosphere, leaving a peak in between which is significantly more prevalent in March – May (MAM) and June – August (JJA). As there is relatively little photosynthesis in the December – February (DJF) and MAM periods, OCS builds up in the atmosphere, followed by net removal throughout JJA and September

https://doi.org/10.5194/acp-2022-215
Preprint. Discussion started: 29 March 2022


Atmospheric Chemistry and Physics Discussions

– November (SON). Despite NH photosynthesis beginning slightly before JJA, there is a clear lag in removing OCS from the upper troposphere. The seasonal peak in OCS in the UTLS region only fully disappears in SON, suggesting there is roughly a 3-month delay on the influence of surface processes on the UTLS ambient mixing ratio. While this fluctuation is driven by seasonality in photosynthesis, the OCS peak is particularly large and extends lower in the atmosphere in the NH ML region, likely as a result of anthropogenic emissions in this region.

The tropopause height is captured adequately by $TOMCAT_{OCS}$ (which is forced by ERA-Interim) and is visible in the homogeneity of the difference around the UTLS. $TOMCAT_{OCS}$ agrees with ACE to within 25 ppt throughout most of the troposphere, which is about 5% of the average estimated atmospheric value of OCS (484 ppt) (Montzka et al., 2007). Similar to the seasonal pattern visible in ACE, the tropospheric OCS mixing ratio in $TOMCAT_{OCS}$ peaks before the NH growing season, MAM. The peak in $TOMCAT_{OCS}$ is lower than ACE can measure, around 5 or 6 km (around 50 – 70°N) and is overestimated compared to ACE, persisting through most of the year. The overestimation in the NH ML is broadly contained within a discrepancy of 25 – 50 ppt from ACE, with the exception of a few anomalies in MAM and JJA, potentially attributed to slower surface OCS uptake or overestimated anthropogenic emissions in this region. The rate of removal of OCS is not quick enough between MAM and JJA to match the measurements exactly. This positive bias in the model below 10 km in the SH throughout DJF and MAM is probably unrelated to the NH positive model bias and would likely be resolved by weaker oceanic emission in the SH, despite already having been reduced by 40% (Suntharalingam et al., 2008).

https://doi.org/10.5194/acp-2022-215
Preprint. Discussion started: 29 March 2022

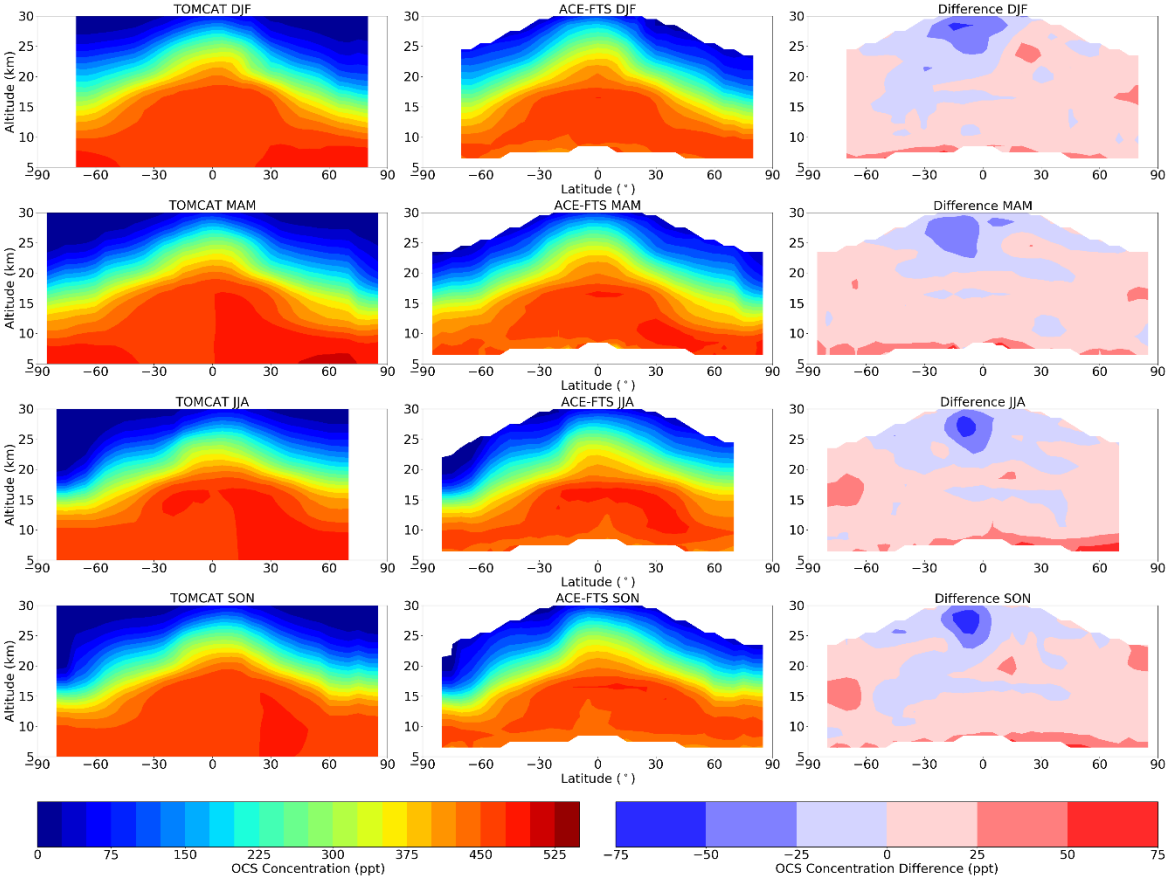

Figure 2. Seasonal zonal mean concentration (mixing ratio) of OCS (ppt) from TOMCAT$_{OCS}$ (left), ACE (centre) and the difference between the two (TOMCAT$_{OCS}$ minus ACE, right) for the period of 2004 to 2018. TOMCAT$_{OCS}$ and ACE data averaged in 5-degree latitude bins and over all longitudes.

Differences between the model and observations in the stratosphere are broadly similar to those in the troposphere and are within ±25 ppt. However, there is considerable model underestimation at 24.5 – 30.5 km between 0° and 30°S, of up to 65 ppt. This region shows a mean seasonal underestimation of between 24.6% and 18.6%, with a peak difference in JJA of 47.5% around 29.5 km at 10°S. As this feature does not follow the pattern of the inter-tropical convergence zone shifting with the hemispheric summertime period, it is unlikely that vertical fluxes are underestimated. The declining gradient in the stratosphere is steeper in the model than in ACE, which suggests that more OCS is being destroyed via photochemical processes in the model than in reality.

Figure 3 shows TOMCAT$_{OCS}$ profiles (blue) in 30° latitude seasonal bins compared to ACE (red), including the standard deviation (shown as error bars) of ACE at each altitude. It is clear the model replicates the vertical structure of OCS, when compared to observed OCS profiles from ACE-FTS. The negative discrepancy in the SH tropical stratosphere, visible in Fig. 2 and discussed above, can be seen in the third row of Fig. 3, as TOMCAT$_{OCS}$ deviates from ACE from 20 km up to 30 km.

https://doi.org/10.5194/acp-2022-215
Preprint. Discussion started: 29 March 2022

Atmospheric Chemistry and Physics Discussions

However, as it remains within the uncertainty of ACE throughout the entire profile, this suggests the upper atmospheric sinks are modelled well by TOMCAT$_{OCS}$. This applies to most of the profiles compared in Fig. 3, in that the modelled TOMCAT$_{OCS}$ profiles generally remain within the standard deviation of ACE-FTS observations. The positive model biases in the both hemispheres below 10 km in Fig. 2 can be seen in Fig. 3, such that the trend at these altitudes in TOMCAT$_{OCS}$ generally does not match ACE. Between 30°S and 90°N, ACE shows a depletion in OCS towards the surface from as high as 15 km – driven by surface uptake. Where a more neutral or increasing gradient between 90°S and 30°S is seen, as there is minimal vegetative uptake and a seasonal cycle strongly influenced by oceanic emission in this region (see Fig. 1).

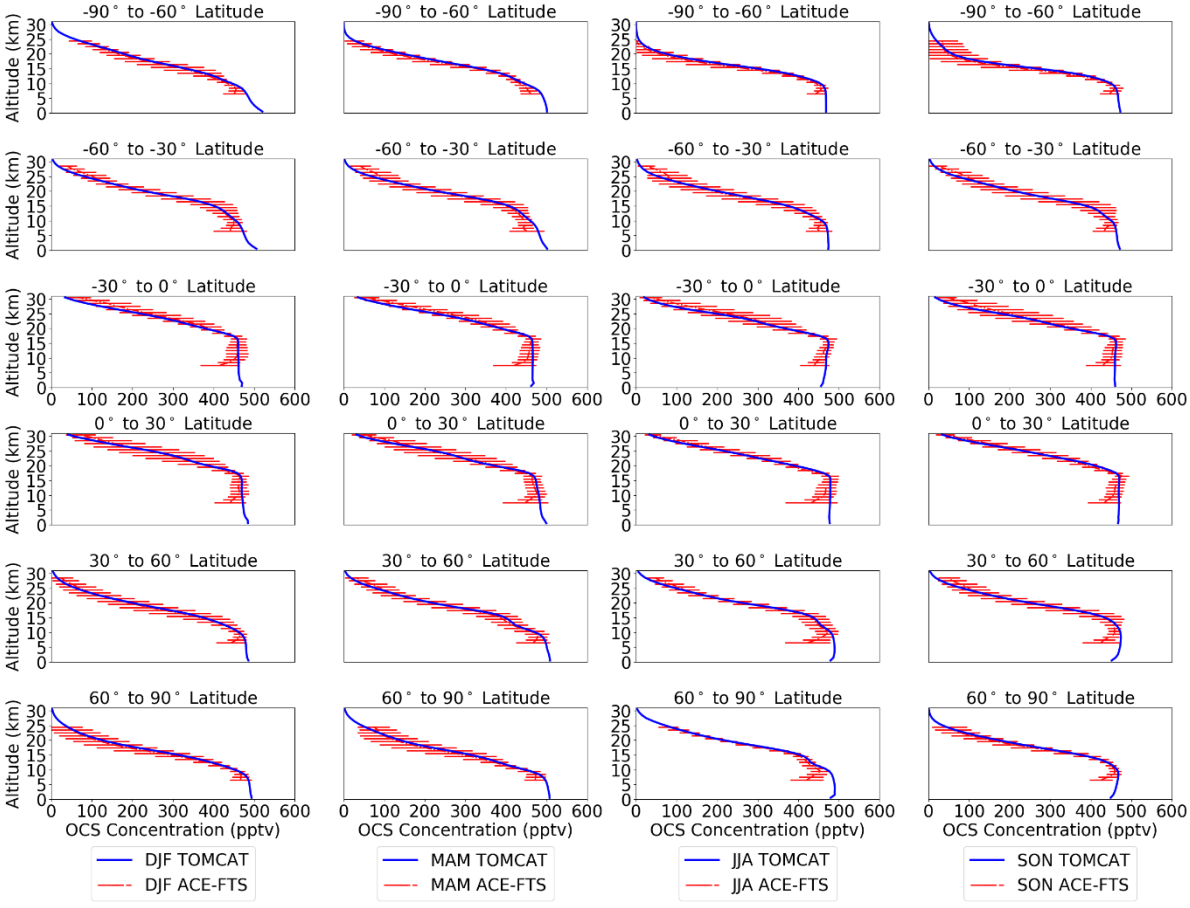

Figure 3. Seasonal mean vertical profiles of OCS concentration (mixing ratio, ppt) from TOMCAT model output (blue) and ACE (red) for six different latitude regions. The error bars are standard deviation of ACE at each altitude level. All profiles are seasonal averages between the years 2004 to 2018.

5 Discussion

After a 10-year spin-up period, the TOMCAT$_{OCS}$ simulations of atmospheric OCS concentrations and the vegetative flux, which are dependent on one another in the model, are in equilibrium between 2004 and 2018. By utilizing a GPP dataset, we

https://doi.org/10.5194/acp-2022-215
Preprint. Discussion started: 29 March 2022


Atmospheric Chemistry and Physics Discussions

estimate mean yearly vegetative OCS uptake of 629 Gg S yr^{-1}, which agrees within the range and uncertainty of the magnitude of this flux from previous studies (see Table 2). The total vegetative and soil sinks agree with findings from Berry et al. (2013) and inversion studies by Kuai et al. (2015) and Ma et al. (2021) to within approximately 150 Gg S yr^{-1} (15%). We balance the OCS budget by implementing an enlarged CS_2 emission source, for the exclusive reason that it is focused over the tropics (Kettle et al., 2002), rather than it being a flux originating from oxidized CS_2. Bottom-up estimates recommend a constraint on global oceanic emission of OCS to approximately 285 – 350 Gg S yr^{-1} (Lennartz et al., 2017, 2021), significantly lower than the fluxes required to bring the budget into balance and bringing our tropical ocean estimate into question. It is clear that tropical fluxes are still uncertain, however inverse modelling of OCS fluxes shows that some combination of a larger tropical oceanic source and vegetative sink resolves the budget and produces adequate model comparison with independent observations (Ma et al., 2021; Remaud et al., 2022), as it does in this work.

A model comparison with surface flask observations shows the OCS budget proposed used to calculate $TOMCAT_{OCS}$ reduces RMSE compared to the control, $TOMCAT_{CON}$, at most sites by approximately 25%, as much as 57% at KUM, but degrading some RMSE, notably at MHD. We have shown improvements in RMSE at NH continental sites, especially the forested sites of LEF and HFM, suggesting utilising GPP to estimate OCS is a suitable option, but there is still moderate underestimation in NH vegetative uptake. This method does have limitations, however, such as calculating OCS uptake using a constant LRU value of 1.6 is not representative of reality, as this deposition ratio is dependent on plant type as well as surface and atmospheric conditions. Our estimation of vegetative uptake in this work does not replicate OCS uptake universally and it is unclear if this is due to localised differences in LRU or on the GPP fields themselves. While soil uptake has been scaled appropriately according to the literature, the distribution is based on work by Kettle et al. (2002) and has since been updated, for example by Ogée et al. (2016). Therefore, it is not possible to conclude misalignment in NH seasonality is due to vegetation or soil exclusively.

The Hawaiin sites, MLO and KUM, show significantly improved RMSE, and some improvement in SCA and phasing, suggesting an enhancement in tropical oceanic emission is reasonable. The lack of OCS measurements in the tropics poses a challenge to both quantifying surface OCS exchange in this region both from a mechanistic perspective and from constraining inverted fluxes (Whelan et al., 2018; Ma et al., 2021; Remaud et al., 2022). While $TOMCAT_{OCS}$ shows an adequate comparison with tropical surface sites and a vertical comparison within the uncertainties of ACE, we acknowledge that no attempt has been made in this work to experiment with reducing tropical surface OCS uptake, which has been suggested as an alternative solution to balance the OCS budget (Ma et al., 2021). Overestimation in SCA at SH sites CGO, PSA and SPO, indicates a reduction in oceanic emissions in this region is necessary, due to the limited continental landmass and associated uptake.

$TOMCAT_{OCS}$ output agrees with ACE-FTS profiles of OCS within 5% throughout the majority of the observed atmosphere (approximately 5 km – 30 km), suggesting the sinks in the upper atmosphere are modelled well, with the exception of some discrepancies in the lower troposphere and the tropical stratosphere. Photochemical destruction is important in our understanding of atmospheric OCS, and due to OH and photolysis loss fields in the stratosphere, the model displays a declining vertical gradient above the tropopause. Our total estimate for this flux is 154 Gg S yr^{-1}, an upward revision of about 40%

https://doi.org/10.5194/acp-2022-215
Preprint. Discussion started: 29 March 2022


Atmospheric Chemistry and Physics Discussions

compared to the previous work of Kettle et al. (2002) and larger than all other estimates in Table 2. This is likely cause of the underestimation in the tropical stratosphere in $TOMCAT_{OCS}$.

Comparison of $TOMCAT_{OCS}$ with ACE profiles shows an excellent representation of the free troposphere, suggesting that we have found a suitable balance of fluxes at the surface, the spatial variability of which requires improvement. Using more recent bottom-up calculations of surface OCS fluxes is a sensible next step. Overestimation in the NH ML region in JJA and SON suggests that anthropogenic emissions could be slightly overestimated or that surface uptake does not initialise quick enough or strong enough to remove OCS from the atmosphere at the start of the growing season.

6 Conclusions

An atmospheric three-dimensional model setup (TOMCAT) was used to test the validity of utilising GPP as a proxy for photosynthetic uptake of OCS on a global scale (Sandoval-Soto and Stanimirov, 2005), by comparing updated and control simulations ($TOMCAT_{OCS}$ and $TOMCAT_{CON}$) to surface flask observations. We have assessed the accuracy of a unique array of fluxes, derived from previous studies (Watts, 2000; Kettle et al., 2002; Suntharalingam et al., 2008; Stimler et al., 2012; Berry et al., 2013; Kuai et al., 2015) and scaled appropriately to fit with the photosynthetic flux calculated in this work, by comparing full global tropospheric and stratospheric model output with limb sounding observations from ACE-FTS. This study is novel in the extended time period analysed and the quality of vertical comparison with measurements. Furthermore, the model's ability to capture the vertical profiles of OCS globally when compared to ACE-FTS profiles shows promise for future OCS work using TOMCAT.

$TOMCAT_{OCS}$ produces a seasonal cycle at the surface that generally captures that from measurements made by the NOAA-ESRL network. Mean SCA across all 14 sites are within ±33.6% of the measurements. The simulation using the full flux inventory from the study by Kettle et al. (2002), $TOMCAT_{CON}$ quantified the improvements in $TOMCAT_{OCS}$ due to using GPP as a proxy for OCS vegetative uptake, at the surface. The amplitude of the seasonal cycle of $TOMCAT_{CON}$ deviates from the flask measurements by an average of ±40.5% across all 14 sites, indicating that our updated fluxes are an improvement.

Disagreement in $TOMCAT_{OCS}$ at the surface compared to NOAA-ESRL observations can be attributed in part to an out-of-date array of fluxes, especially so for soil fields and oceanic emissions. Use of more recent bottom-up estimates would be a next step in this work. However, this presents the challenge that this may not necessarily guarantee a closed budget, which is the case in the prior flux estimates utilised by Ma et al. (2021). The use of GPP has clearly shown improvements compared to the OCS vegetative uptake fields from Kettle et al. (2002), however some substantial changes are necessary in future, such as using inter-annually varying GPP and CO_2 mixing ratios, as well as a temporally and spatially resolved LRU. The latter of these 3 changes is an exceptionally challenging and lengthy endeavour due to its dependence on plant type, soil and atmospheric conditions, hence an initial step would be just to vary LRU based on ecosystem on a continental or country scale. Advances are being made in this area, with mechanistic and LRU approaches emerging that reduce uncertainty in OCS vegetative uptake (Maignan et al., 2021). The use of an enhanced tropical ocean source is justified in this work by offering

https://doi.org/10.5194/acp-2022-215
Preprint. Discussion started: 29 March 2022


Atmospheric Chemistry and Physics Discussions

suitable satellite and surface observational comparisons. However, we acknowledge that oceanic emissions alone may not account for this discrepancy and based on $TOMCAT_{OCS}$ performance at MLO and KUM, this is not a perfect solution for balancing the global OCS budget.

While we have shown that $TOMCAT_{OCS}$ compares well with satellite observations, the region between the surface and approximately 6 km, which is not measure by ACE-FTS, could hold a lot of information useful in resolving surface fluxes. Measurements at the surface are sensitive to minor flux changes, although in the well-mixed mid to upper troposphere these spatial changes are less important. Validation of model output to ground-based Fourier Transform spectrometer column OCS measurements could improve our understanding and ability to model the lower troposphere. Furthermore, incorporating measurements with vertical information into inversion schemes has been shown to improve the posterior OCS fluxes, specifically using HIPPO flight data (Ma et al., 2021). Therefore, further study following on from this work will be to derive an a posteriori set of fluxes using an inversion scheme based on an up-to-date prior, and surface observations and a dataset containing vertical information near the surface.

Code and Data Availability

Anthropogenic OCS emission data are available at https://portal.nersc.gov/project/m2319/ (Campbell, 2022; Zumkehr et al., 2018). GPP dataset is available at https://datashare.ed.ac.uk/handle/10283/2080 (Slevin et al., 2016). ACE-FTS data are available at http://www.ace.uwaterloo.ca/data.php (ACE-FTS, 2022). NOAA-ESRL surface flask measurements of OCS are available at https://www.esrl.noaa.gov/gmd/dv/data/ (ESRL Global Monitoring Laboratory, 2022). Model data are available at https://doi.org/10.5281/zenodo.6368542.

Author Contribution

Model runs and data analysis were performed by MPCar, with support from RJP. JJH and MPChi designed the study. CJW provided the CO_2 model data. Control OCS emissions were provided by PS. TOMCAT model is maintained and updated by the team at the University of Leeds: MPChi, WF, CJW and RJP. Manuscript was written by MPCar, with contributions from all co-authors.

Competing Interests

The authors declare that they have no conflict of interest.

https://doi.org/10.5194/acp-2022-215
Preprint. Discussion started: 29 March 2022

Atmospheric Chemistry and Physics Discussions

Acknowledgements

Computation and data analysis were carried out on the ARC computing system at Leeds and the ALICE/SPECTRE system at Leicester. The authors thank P. Bernath for access to ACE-FTS satellite observations, D. Slevin, S. Tett and M. Williams for access to GPP data from JULES and S. Montzka and J. Elkins and other contributors from NOAA for providing the flask measurements.

Financial support

MPCar thanks the Leicester Institute of Space and Earth Observation, for providing a studentship at the University of Leicester. This study was funded as part of the UK Research and Innovation Natural Environment Research Council's support of the National Centre for Earth Observation, contract number PR140015.

References

ACE-FTS: ACE Data – Atmospheric Chemistry Experiment, available at: http://www.ace.uwaterloo.ca/data.php, last access: 14 March 2022.

Barkley, M. P., Palmer, P. I., Boone, C. D., Bernath, P. F., and Suntharalingam, P.: Global distributions of carbonyl sulfide in the upper troposphere and stratosphere, Geophys. Res. Lett., 35, L14810, https://doi.org/10.1029/2008GL034270, 2008.

Barnes, I., Becker, K. H., and Patroescu, I.: The tropospheric oxidation of dimethyl sulfide: A new source of carbonyl sulfide, 21, 2389–2392, https://doi.org/10.1029/94GL02499, 1994.

Bernath, P. F.: The Atmospheric Chemistry Experiment (ACE), J. Quant. Spectrosc. Radiat. Transfer, 186, 3–16, https://doi.org/10.1016/j.jqsrt.2016.04.006, 2017.

Bernath, P. F., McElroy, C. T., Abrams, M. C., Boone, C. D., Butler, M., Camy-Peyret, C., Carleer, M., Clerbaux, C., Coheur, P.-F., Colin, R., DeCola, P., DeMazière, M., Drummond, J. R., Dufour, D., Evans, W. F. J., Fast, H., Fussen, D., Gilbert, K., Jennings, D. E., Llewellyn, E. J., Lowe, R. P., Mahieu, E., McConnell, J. C., McHugh, M., McLeod, S. D., Michaud, R., Midwinter, C., Nassar, R., Nichitiu, F., Nowlan, C., Rinsland, C. P., Rochon, Y. J., Rowlands, N., Semeniuk, K., Simon, P., Skelton, R., Sloan, J. J., Soucy, M.-A., Strong, K., Tremblay, P., Turnbull, D., Walker, K. A., Walkty, I., Wardle, D. A., Wehrle, V., Zander, R., and Zou, J.: Atmospheric Chemistry Experiment (ACE): Mission overview, 32, https://doi.org/10.1029/2005GL022386, 2005.

Berry, J., Wolf, A., Campbell, J. E., Baker, I., Blake, N., Blake, D., Denning, A. S., Kawa, S. R., Montzka, S. A., Seibt, U., Stimler, K., Yakir, D., and Zhu, Z.: A coupled model of the global cycles of carbonyl sulfide and CO_2: A possible new window on the carbon cycle, J. Geophys. Res. Biogeosci., 118, 842–852, https://doi.org/10.1002/jgrg.20068, 2013.

Blonquist, J. M., Montzka, S. A., Munger, J. W., Yakir, D., Desai, A. R., Dragoni, D., Griffis, T. J., Monson, R. K., Scott, R. L., and Bowling, D. R.: The potential of carbonyl sulfide as a proxy for gross primary production at flux tower sites, 116, https://doi.org/10.1029/2011JG001723, 2011.

Boone, C. D. and Bernath, P. F.: The instrumental line shape of the atmospheric chemistry experiment Fourier transform spectrometer (ACE-FTS), Journal of Quantitative Spectroscopy and Radiative Transfer, 230, 1–12, https://doi.org/10.1016/j.jqsrt.2019.03.018, 2019.

Boone, C. D., Bernath, P. F., Cok, D., Jones, S. C., and Steffen, J.: Version 4 retrievals for the atmospheric chemistry experiment Fourier transform spectrometer (ACE-FTS) and imagers, Journal of Quantitative Spectroscopy and Radiative Transfer, 247, 106939, https://doi.org/10.1016/j.jqsrt.2020.106939, 2020.

Campbell, J. E.: Campbell Lab Data Sharing, available at: https://portal.nersc.gov/project/m2319/, last access: 14 March 2022.

Campbell, J. E., Carmichael, G. R., Chai, T., Mena-Carrasco, M., Tang, Y., Blake, D. R., Blake, N. J., Vay, S. A., Collatz, G. J., Baker, I., Berry, J. A., Montzka, S. A., Sweeney, C., Schnoor, J. L., and Stanier, C. O.: Photosynthetic Control of Atmospheric Carbonyl Sulfide During the Growing Season, Sci., 322, 1085–1088, https://doi.org/10.1126/science.1164015, 2008.

Chen, M., Rafique, R., Asrar, G. R., Bond-Lamberty, B., Ciais, P., Zhao, F., Reyer, C. P. O., Ostberg, S., Chang, J., Ito, A., Yang, J., Zeng, N., Kalnay, E., West, T., Leng, G., Francois, L., Munhoven, G., Henrot, A., Tian, H., Pan, S., Nishina, K., Viovy, N., Morfopoulos, C., Betts, R., Schaphoff, S., Steinkamp, J., and Hickler, T.: Regional contribution to variability and trends of global gross primary productivity, Environ. Res. Lett., 12, 105005, https://doi.org/10.1088/1748-9326/aa8978, 2017.

Chin, M. and Davis, D., D.: Global sources and sinks of OCS and CS_2 and their distributions, Global Biogeochem. Cycles, 7, 321–337, https://doi.org/10.1029/93GB00568, 1993.

Chipperfield, M. P.: New version of the TOMCAT/SLIMCAT off-line chemical transport model: Intercomparison of stratospheric tracer experiments, 132, 1179–1203, https://doi.org/10.1256/qj.05.51, 2006.

Claxton, T., Hossaini, R., Wild, O., Chipperfield, M. P., and Wilson, C.: On the Regional and Seasonal Ozone Depletion Potential of Chlorinated Very Short-Lived Substances, 46, 5489–5498, https://doi.org/10.1029/2018GL081455, 2019.

Crutzen, P. J.: The possible importance of CSO for the sulfate layer of the stratosphere, Geophys. Res. Lett., 3, 73–76, https://doi.org/10.1029/GL003i002p00073, 1976.

Dee, D. P., Uppala, S. M., Simmons, A. J., Berrisford, P., Poli, P., Kobayashi, S., Andrae, U., Balmaseda, M. A., Balsamo, G., Bauer, P., Bechtold, P., Beljaars, A. C. M., Berg, L. van de, Bidlot, J., Bormann, N., Delsol, C., Dragani, R., Fuentes, M., Geer, A. J., Haimberger, L., Healy, S. B., Hersbach, H., Hólm, E. V., Isaksen, L., Kållberg, P., Köhler, M., Matricardi, M., McNally, A. P., Monge-Sanz, B. M., Morcrette, J.-J., Park, B.-K., Peubey, C., Rosnay, P. de, Tavolato, C., Thépaut, J.-N., and Vitart, F.: The ERA-Interim reanalysis: configuration and performance of the data assimilation system, 137, 553–597, https://doi.org/10.1002/qj.828, 2011.

https://doi.org/10.5194/acp-2022-215
Preprint. Discussion started: 29 March 2022


Atmospheric Chemistry and Physics Discussions

Duncan, B. N., Martin, R. V., Staudt, A. C., Yevich, R., and Logan, J. A.: Interannual and seasonal variability of biomass burning emissions constrained by satellite observations, 108, ACH 1-1-ACH 1-22, https://doi.org/10.1029/2002JD002378, 2003.

ESRL Global Monitoring Laboratory - FTP Navigator: https://gml.noaa.gov/dv/data/, last access: 14 March 2022.

Feng, W., Chipperfield, M. P., Dhomse, S., Monge-Sanz, B. M., Yang, X., Zhang, K., and Ramonet, M.: Evaluation of cloud convection and tracer transport in a three-dimensional chemical transport model, 21, 2011.

Fung, I. Y., Tucker, C. J., and Prentice, K. C.: Application of Advanced Very High Resolution Radiometer vegetation index to study atmosphere-biosphere exchange of CO_2, 92, 2999–3015, https://doi.org/10.1029/JD092iD03p02999, 1987.

Glatthor, N., Höpfner, M., Baker, I. T., Berry, J., Campbell, J. E., Kawa, S. R., Krysztofiak, G., Leyser, A., Sinnhuber, B.-M., Stiller, G. P., Stinecipher, J., and Clarmann, T. von: Tropical sources and sinks of carbonyl sulfide observed from space, Geophys. Res. Lett., 42, 10,082-10,090, https://doi.org/10.1002/2015GL066293, 2015.

Glatthor, N., Höpfner, M., Leyser, A., Stiller, G. P., von Clarmann, T., Grabowski, U., Kellmann, S., Linden, A., Sinnhuber, B.-M., Krysztofiak, G., and Walker, K. A.: Global carbonyl sulfide (OCS) measured by MIPAS/Envisat during 2002–2012, Atmos. Chem. Phys., 17, 2631–2652, https://doi.org/10.5194/acp-17-2631-2017, 2017.

Gloor, E., Wilson, C., Chipperfield, M. P., Chevallier, F., Buermann, W., Boesch, H., Parker, R., Somkuti, P., Gatti, L. V., Correia, C., Domingues, L. G., Peters, W., Miller, J., Deeter, M. N., and Sullivan, M. J. P.: Tropical land carbon cycle responses to 2015/16 El Niño as recorded by atmospheric greenhouse gas and remote sensing data, 373, 20170302, https://doi.org/10.1098/rstb.2017.0302, 2018.

Gordon, I. E., Rothman, L. S., Hill, C., Kochanov, R. V., Tan, Y., Bernath, P. F., Birk, M., Boudon, V., Campargue, A., Chance, K. V., Drouin, B. J., Flaud, J.-M., Gamache, R. R., Hodges, J. T., Jacquemart, D., Perevalov, V. I., Perrin, A., Shine, K. P., Smith, M.-A. H., Tennyson, J., Toon, G. C., Tran, H., Tyuterev, V. G., Barbe, A., Császár, A. G., Devi, V. M., Furtenbacher, T., Harrison, J. J., Hartmann, J.-M., Jolly, A., Johnson, T. J., Karman, T., Kleiner, I., Kyuberis, A. A., Loos, J., Lyulin, O. M., Massie, S. T., Mikhailenko, S. N., Moazzen-Ahmadi, N., Müller, H. S. P., Naumenko, O. V., Nikitin, A. V., Polyansky, O. L., Rey, M., Rotger, M., Sharpe, S. W., Sung, K., Starikova, E., Tashkun, S. A., Auwera, J. V., Wagner, G., Wilzewski, J., Wcisło, P., Yu, S., and Zak, E. J.: The HITRAN2016 molecular spectroscopic database, Journal of Quantitative Spectroscopy and Radiative Transfer, 203, 3–69, https://doi.org/10.1016/j.jqsrt.2017.06.038, 2017.

Huijnen, V., Williams, J., van Weele, M., van Noije, T., Krol, M., Dentener, F., Segers, A., Houweling, S., Peters, W., de Laat, J., Boersma, F., Bergamaschi, P., van Velthoven, P., Le Sager, P., Eskes, H., Alkemade, F., Scheele, R., Nédélec, P., and Pätz, H.-W.: The global chemistry transport model TM5: description and evaluation of the tropospheric chemistry version 3.0, 3, 445–473, https://doi.org/10.5194/gmd-3-445-2010, 2010.

Kato, H., Saito, M., Nagahata, Y., and Katayama, Y.: Degradation of ambient carbonyl sulfide by Mycobacterium spp. in soil, 154, 249–255, https://doi.org/10.1099/mic.0.2007/011213-0, 2008.

Kesselmeier, J., Teusch, N., and Kuhn, U.: Controlling variables for the uptake of atmospheric carbonyl sulfide by soil, 104, 11577–11584, https://doi.org/10.1029/1999JD900090, 1999.

Kettle, A. J. and Andreae, M. O.: Flux of dimethylsulfide from the oceans: A comparison of updated data sets and flux models, 105, 26793–26808, https://doi.org/10.1029/2000JD900252, 2000.

Kettle, A. J., Kuhn, U., Hobe, M. von, Kesselmeier, J., and Andreae, M. O.: Global budget of atmospheric carbonyl sulfide: Temporal and spatial variations of the dominant sources and sinks, J. Geophys. Res., 107, ACH 25-1-ACH 25-16, https://doi.org/10.1029/2002JD002187, 2002.

Kremser, S., Jones, N. B., Palm, M., Lejeune, B., Wang, Y., Smale, D., and Deutscher, N. M.: Positive trends in Southern Hemisphere carbonyl sulfide, Geophys. Res. Lett., 42, 9473–9480, https://doi.org/10.1002/2015GL065879, 2015.

Kremser, S., Thomason, L. W., Hobe, M. von, Hermann, M., Deshler, T., Timmreck, C., Toohey, M., Stenke, A., Schwarz, J. P., Weigel, R., Fueglistaler, S., Prata, F. J., Vernier, J.-P., Schlager, H., Barnes, J. E., Antuña-Marrero, J.-C., Fairlie, D., Palm, M., Mahieu, E., Notholt, J., Rex, M., Bingen, C., Vanhellemont, F., Bourassa, A., Plane, J. M. C., Klocke, D., Carn, S. A., Clarisse, L., Trickl, T., Neely, R., James, A. D., Rieger, L., Wilson, J. C., and Meland, B.: Stratospheric aerosol—Observations, processes, and impact on climate, 54, 278–335, https://doi.org/10.1002/2015RG000511, 2016.

Kuai, L., Worden, J. R., Campbell, J. E., Kulawik, S. S., Li, K.-F., Lee, M., Weidner, R. J., Montzka, S. A., Moore, F. L., Berry, J. A., Baker, I., Denning, A. S., Bian, H., Bowman, K. W., Liu, J., and Yung, Y. L.: Estimate of carbonyl sulfide tropical oceanic surface fluxes using Aura Tropospheric Emission Spectrometer observations, J. Geophys.Res. Atmos., 120, 11,012-11,023, https://doi.org/10.1002/2015JD023493, 2015.

Launois, T., Belviso, S., Bopp, L., Fichot, C. G., and Peylin, P.: A new model for the global biogeochemical cycle of carbonyl sulfide - Part 1: Assessment of direct marine emissions with an oceanic general circulation and biogeochemistry model, 15, 2295–2312, https://doi.org/10.5194/acp-15-2295-2015, 2015a.

Launois, T., Peylin, P., Belviso, S., and Poulter, B.: A new model of the global biogeochemical cycle of carbonyl sulfide – Part 2: Use of carbonyl sulfide to constrain gross primary productivity in current vegetation models, 15, 9285–9312, https://doi.org/10.5194/acp-15-9285-2015, 2015b.

Lejeune, B., Mahieu, E., Vollmer, M. K., Reimann, S., Bernath, P. F., Boone, C. D., Walker, K. A., and Servais, C.: Optimized approach to retrieve information on atmospheric carbonyl sulfide (OCS) above the Jungfraujoch station and change in its abundance since 1995, J. Quant. Spectrosc. Radiat. Transfer, 186, 81–95, https://doi.org/10.1016/j.jqsrt.2016.06.001, 2017.

Lennartz, S. T., Marandino, C. A., von Hobe, M., Cortes, P., Quack, B., Simo, R., Booge, D., Pozzer, A., Steinhoff, T., Arevalo-Martinez, D. L., Kloss, C., Bracher, A., Röttgers, R., Atlas, E., and Krüger, K.: Direct oceanic emissions unlikely to account for the missing source of atmospheric carbonyl sulfide, 17, 385–402, https://doi.org/10.5194/acp-17-385-2017, 2017.

Lennartz, S. T., Gauss, M., von Hobe, M., and Marandino, C. A.: Monthly resolved modelled oceanic emissions of carbonyl sulphide and carbon disulphide for the period 2000–2019, 13, 2095–2110, https://doi.org/10.5194/essd-13-2095-2021, 2021.

Li, W., Yu, L., Yuan, D., Wu, Y., and Zeng, X.: A study of the activity and ecological significance of carbonic anhydrase from soil and its microbes from different karst ecosystems of Southwest China, Plant Soil, 272, 133–141, https://doi.org/10.1007/s11104-004-4335-9, 2005.

Ma, J., Kooijmans, L. M. J., Cho, A., Montzka, S. A., Glatthor, N., Worden, J. R., Kuai, L., Atlas, E. L., and Krol, M. C.: Inverse modelling of carbonyl sulfide: implementation, evaluation and implications for the global budget, Atmos. Chem. Phys., 21, 3507–3529, https://doi.org/10.5194/acp-21-3507-2021, 2021.

Maignan, F., Abadie, C., Remaud, M., Kooijmans, L. M. J., Kohonen, K.-M., Commane, R., Wehr, R., Campbell, J. E., Belviso, S., Montzka, S. A., Raoult, N., Seibt, U., Shiga, Y. P., Vuichard, N., Whelan, M. E., and Peylin, P.: Carbonyl sulfide: comparing a mechanistic representation of the vegetation uptake in a land surface model and the leaf relative uptake approach, 18, 2917–2955, https://doi.org/10.5194/bg-18-2917-2021, 2021.

Maseyk, K., Berry, J. A., Billesbach, D., Campbell, J. E., Torn, M. S., Zahniser, M., and Seibt, U.: Sources and sinks of carbonyl sulfide in an agricultural field in the Southern Great Plains, PNAS, 111, 9064–9069, https://doi.org/10.1073/pnas.1319132111, 2014.

McNorton, J., Wilson, C., Gloor, M., Parker, R. J., Boesch, H., Feng, W., Hossaini, R., and Chipperfield, M. P.: Attribution of recent increases in atmospheric methane through 3-D inverse modelling, 18, 18149–18168, https://doi.org/10.5194/acp-18-18149-2018, 2018.

Monks, S. A., Arnold, S. R., Hollaway, M. J., Pope, R. J., Wilson, C., Feng, W., Emmerson, K. M., Kerridge, B. J., Latter, B. L., Miles, G. M., Siddans, R., and Chipperfield, M. P.: The TOMCAT global chemical transport model v1.6: description of chemical mechanism and model evaluation, Geosci. Model Dev., 10, 3025–3057, https://doi.org/10.5194/gmd-10-3025-2017, 2017.

Montzka, S. A., Calvert, P., Hall, B. D., Elkins, J. W., Conway, T. J., Tans, P. P., and Sweeney, C.: On the global distribution, seasonality, and budget of atmospheric carbonyl sulfide (COS) and some similarities to CO_2, J. Geophys. Res., 112, https://doi.org/10.1029/2006JD007665, 2007.

Ogée, J., Sauze, J., Kesselmeier, J., Genty, B., Van Diest, H., Launois, T., and Wingate, L.: A new mechanistic framework to predict OCS fluxes from soils, Biogeosciences, 13, 2221–2240, https://doi.org/10.5194/bg-13-2221-2016, 2016.

Parker, R. J., Boesch, H., McNorton, J., Comyn-Platt, E., Gloor, M., Wilson, C., Chipperfield, M. P., Hayman, G. D., and Bloom, A. A.: Evaluating year-to-year anomalies in tropical wetland methane emissions using satellite CH4 observations, Remote Sensing of Environment, 211, 261–275, https://doi.org/10.1016/j.rse.2018.02.011, 2018.

Protoschill-Krebs, G. and Kesselmeier, J.: Enzymatic Pathways for the Consumption of Carbonyl Sulphide (COS) by Higher Plants*, 105, 206–212, https://doi.org/10.1111/j.1438-8677.1992.tb00288.x, 1992.

Protoschill-Krebs, G., Wilhelm, C., and Kesselmeier, J.: Consumption of carbonyl sulphide (COS) by higher plant carbonic anhydrase (CA), 30, 3151–3156, https://doi.org/10.1016/1352-2310(96)00026-X, 1996.

Remaud, M., Chevallier, F., Maignan, F., Belviso, S., Berchet, A., Parouffe, A., Abadie, C., Bacour, C., Lennartz, S., and Peylin, P.: Plant gross primary production, plant respiration and carbonyl sulfide emissions over the globe inferred by atmospheric inverse modelling, Atmos. Chem. Phys., 22, 2525–2552, https://doi.org/10.5194/acp-22-2525-2022, 2022.

Sandoval-Soto, L. and Stanimirov, M.: Global uptake of carbonyl sulfide (COS) by terrestrial vegetation: Estimates corrected by deposition velocities normalized to the uptake of carbon dioxide (CO_2), 8, 2005.

630 Seibt, U., Wingate, L., Lloyd, J., and Berry, J. A.: Diurnally variable δ18O signatures of soil CO_2 fluxes indicate carbonic anhydrase activity in a forest soil, 111, https://doi.org/10.1029/2006JG000177, 2006.

Sellers, P. J., Meeson, B. W., Hall, F. G., Asrar, G., Murphy, R. E., Schiffer, R. A., Bretherton, F. P., Dickinson, R. E., Ellingson, R. G., Field, C. B., Huemmrich, K. F., Justice, C. O., Melack, J. M., Roulet, N. T., Schimel, D. S., and Try, P. D.: Remote sensing of the land surface for studies of global change: Models — algorithms — experiments, Remote Sensing of
635 Environment, 51, 3–26, https://doi.org/10.1016/0034-4257(94)00061-Q, 1995.

Slevin, D., Tett, S., and Williams, M.: Global GPP simulated by the JULES land surface model for 2001-2010, https://doi.org/10.7488/ds/1461, 2016.

Spivakovsky, C. M., Logan, J. A., Montzka, S. A., Balkanski, Y. J., Foreman-Fowler, M., Jones, D. B. A., Horowitz, L. W., Fusco, A. C., Brenninkmeijer, C. a. M., Prather, M. J., Wofsy, S. C., and McElroy, M. B.: Three-dimensional climatological
640 distribution of tropospheric OH: Update and evaluation, 105, 8931–8980, https://doi.org/10.1029/1999JD901006, 2000.

Stimler, K., Berry, J. A., and Yakir, D.: Effects of Carbonyl Sulfide and Carbonic Anhydrase on Stomatal Conductance, 158, 524–530, https://doi.org/10.1104/pp.111.185926, 2012.

Sun, W., Kooijmans, L. M. J., Maseyk, K., Chen, H., Mammarella, I., Vesala, T., Levula, J., Keskinen, H., and Seibt, U.: Soil fluxes of carbonyl sulfide (COS), carbon monoxide, and carbon dioxide in a boreal forest in southern Finland, 18, 1363–1378,
645 https://doi.org/10.5194/acp-18-1363-2018, 2018.

Suntharalingam, P., Kettle, A. J., Montzka, S. M., and Jacob, D. J.: Global 3-D model analysis of the seasonal cycle of atmospheric carbonyl sulfide: Implications for terrestrial vegetation uptake, Geophys. Res. Lett., 35, 6, https://doi.org/10.1029/2008GL034332, 2008.

Watts, S. F.: The mass budgets of carbonyl sulfide, dimethyl sulfide, carbon disulfide and hydrogen sulfide, 34, 19, 2000.

650 Whelan, M. E., Lennartz, S. T., Gimeno, T. E., Wehr, R., Wohlfahrt, G., Wang, Y., Kooijmans, L. M. J., Hilton, T. W., Belviso, S., Peylin, P., Commane, R., Sun, W., Chen, H., Kuai, L., Mammarella, I., Maseyk, K., Berkelhammer, M., Li, K.-F., Yakir, D., Zumkehr, A., Katayama, Y., Ogée, J., Spielmann, F. M., Kitz, F., Rastogi, B., Kesselmeier, J., Marshall, J., Erkkilä, K.-M., Wingate, L., Meredith, L. K., He, W., Bunk, R., Launois, T., Vesala, T., Schmidt, J. A., Fichot, C. G., Seibt, U., Saleska, S., Saltzman, E. S., Montzka, S. A., Berry, J. A., and Campbell, J. E.: Reviews and Syntheses: Carbonyl Sulfide as a Multi-
655 scale Tracer for Carbon and Water Cycles, 1–97, https://doi.org/10.5194/bg-2017-427, 2018.

Wilson, C., Gloor, M., Gatti, L. V., Miller, J. B., Monks, S. A., McNorton, J., Bloom, A. A., Basso, L. S., and Chipperfield, M. P.: Contribution of regional sources to atmospheric methane over the Amazon Basin in 2010 and 2011, 30, 400–420, https://doi.org/10.1002/2015GB005300, 2016.

Zumkehr, A., Hilton, T. W., Whelan, M., Smith, S., Kuai, L., Worden, J., and Campbell, J. E.: Global gridded anthropogenic
660 emissions inventory of carbonyl sulfide, Atmospheric Environment, 183, 11–19, https://doi.org/10.1016/j.atmosenv.2018.03.063, 2018.